

Numerical modelling of effect of channel width on heat transfer and ventilation in a built-in PV-Trombe wall

Yaxin Su^{1,3}, Bingtao Zhao², Feining Lei¹, Wenyi Deng¹

¹ School of Environment Science and Engineering, Donghua University, Shanghai, China

² School of Energy and Power Engineering, University of Shanghai for Science and Technology, Shanghai, China;

E-mail: suyx@dhu.edu.cn

Abstract. The heat transfer and air flow rate in a built-in PV-Trombe wall with vertical inlet were numerically simulated based on CFD method. Effect of channel width on heat transfer and air flow rate was discussed. As the channel width increased, the natural convective heat transfer was enhanced and the PV surface was better cooled by the air which improved the PV electricity efficiency slightly. The ventilation rate through the built-in PV-Trombe wall reached its maximum at an optimal ratio of the channel width to the channel height, $(b/H)_{opt}=1/5$. Dimensionless expressions to calculate the averaged heat transfer coefficient, Nusselt number, and the air flow rate in term of a Reynolds number were correlated according to a modified Rayleigh number by multivariable regression analysis.

1. Introduction

Buildings will consume about 1/3 of the total energy in the future with the fast development of large cities. It is very important to develop technologies to utilize new and/or renewable energies in order to reduce the dependence of building energy demand on fossil fuels. The integration of solar energy to buildings is a key topic for building energy conservation. Solar chimney and Trombe wall are simple but effective technologies to use solar radiation to enhance the natural ventilation, which could improve the indoor air quality and air-conditioning system [1,2].

Many research results showed that Trombe wall could save building energy. Bojic et al. [3] simulated the building energy with Trombe walls by using EnergyPlus software and showed that the annual final energy saving during heating is around 20% when the building with Trombe walls is used in Lyon, France. Abbassi et al [4] studied the energetic performance of a Trombe wall system under typical Tunisian buildings by TRNSYS software and validated by a small scale experimental prototype. Results showed that 4 m² Trombe wall areas can save up 50% of annually heating auxiliary energy of a simple classical Tunisian building and 77% can be saved with an 8 m² Trombe wall. Briga-Sá et al [5] also concluded that energy heating needs can be reduced 16.36% if a Trombe wall is added to the building envelope in Portugal. Shen et al [6] numerically compared the composite and classical Trombe walls to prove better energetic performances of the composite Trombe wall in cold and/or cloudy weather. Jaber and Ajib [7] studied the thermal, environment and economic impact of Trombe wall system for residential building in Mediterranean region by using Life Cycle Cost (LCC) criterion and concluded that Trombe wall system had a considerable benefit and reduced the annual heating energy consumption.

³ Author to whom any correspondence should be addressed.



However, the conventional Trombe wall could only use the solar energy to improve the indoor ventilation and/or heating/cooling and could not provide both electricity and heating/cooling to the rooms. Ji et al [8-10] proposed a PV-Trombe wall in which the front side of the glazing is composed of photovoltaic panels. So the PV-Trombe wall could convert solar radiation into electricity and heat simultaneously. However, the PV panel on the front cover hinders the penetration of solar rays into the Trombe wall channel between the walls and glazing [11]. Therefore, the efficiency of the Trombe wall is reduced in terms of heat gain [12]. The study by Sun et al [13] revealed that installing PV panels over the glazing reduces the thermal performance of the Trombe wall up to 17%. This reduction is due to the obstructed penetration of the sun's rays into the mass wall. When the glazing was fully covered by PV cells, the total solar utilization rate of the PV-Trombe wall was reduced 5% even when the solar-electricity was taken into account [13]. Koyunbaba and Yilmaz [14] experimentally compared performances of Trombe wall systems with single glass, double glass and PV panels in Izmir, Turkey, where they found that the highest energy saving was achieved by using Trombe wall system with single glass. Numerical results [14] also showed that the air temperature in both the Trombe wall channel and the room dropped when PV panels were installed on the glass cover, which resulted in a decreased ventilation performance.

In order to improve the solar utilization, Su et al [15] proposed a new built-in PV-Trombe wall, in which the PV cells are installed on the absorber wall surface other than the front side of the glazing. The solar radiation penetrates the glass cover and enters the Trombe wall channel. Then the solar radiation is absorbed by the PV cells and partly converted into electricity power. The remained solar heat is transferred to the air via natural convection to form natural ventilation. Compared to the PV-Trombe wall proposed by Ji et al [8-10], the PV cells coverage rate on the absorber wall is 100%, other than the limit of 50% on the glazing.

The heat transfer in the Trombe wall channel is a critical parameter for the calculation of the ventilation rate. The convective heat transfer coefficient is usually calculated by an empirical equation [16]. In this paper, computational fluid dynamics (CFD) simulation was used to calculate the air flow and heat transfer in the built-in PV-Trombe wall channel and the effect of the channel width on the ventilation and heat transfer performance was studied. The dimensionless parameters for the heat transfer coefficient and ventilation rate were finally correlated based on the numerical data for engineering application.

2. Model

2.1. Built-in PV-Trombe wall model

Figure 1 presents the built-in PV-Trombe wall with a vertical inlet, which is made up of a glass cover/glazing, absorber wall and the air channel between the glazing and absorber wall. The monocrystalline PV cell panel is attached to the absorber wall and separated by insulating layer. The channel height is $H=3\text{m}$, the channel width is $b=0.1\text{-}0.9\text{m}$, the thickness of the glass cover is 4mm. Solar radiation passes through the glass cover and impinges on the PV panels. A part of the solar energy is then converted to electricity by the PV cells, e.g., about 10%-15% depending on the cells' efficiency and the remained solar radiation is converted into heat which increases the PV panels' temperature. The air flowing over the PV panels is then heated by natural convection, resulting to the rising flow in the channel due to the buoyancy effect. The heated air generates natural ventilation in the Trombe wall and the PV panels are then effectively cooled by the air flow, as a result, the PV cell efficiency for power generation is maintained due to the cooling by the natural ventilation. When a damper regulator is installed in the channel, the heated air could be introduced into the room for heating in winter. In summer, the inlet of the Trombe wall channel is connected with the room at the bottom and the heated air just flow directly to the open air at the channel top, then the air flow could induce a natural ventilation in the room for cooling. The solar radiation intensity and the heat flux impinging on the PV panels are noted as q_1 and q_2 , respectively. The physical properties of the glass and PV are listed in Table 1.

When the inlet is vertical or horizontal, the air flowing into the cavity will undergo different flow pattern. When a horizontal inlet is designed, there will be a vortex near the inlet, which may influence the local

heat transfer there. However, when the channel height is tall enough, this effect on the overall heat transfer could be just neglected. In the present study, the vertical inlet is used for the calculation.

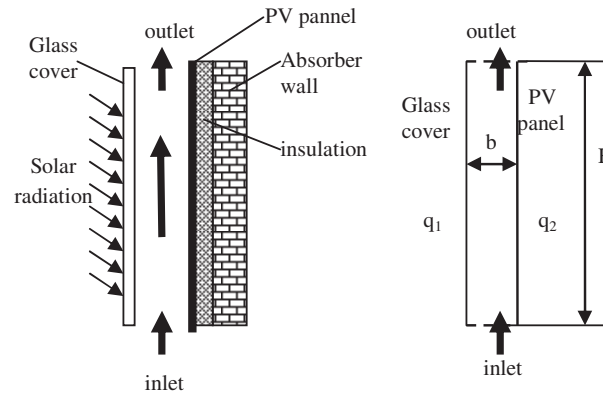


Figure 1 Physical model and simplified model of the built-in PV-Trombe wall

Table 1 Physical properties of the glass and PV

	density (kg/m ³)	Specific heat (J/kg·K)	Thermal conductivity (W/m·K)	thickness (mm)	absorptivity	emissivity	transmittivity
glass	2515	810	1.4	4	0.06	0.79	0.85
PV	2330	712	148	0.3	0.9	0.96	-

2.2. CFD model

The air flow is considered as two dimensional and incompressible flow in the Trombe wall channel. Gan [17] simulated the natural ventilation in typical Trombe wall by CFD and showed that RNG k- ϵ turbulent model was able to predict the data that agreed well with experimental data. The RNG k- ϵ turbulent model was further used to study the air flow and heat transfer in Trombe wall [18-20]. In the present study, RNG k- ϵ turbulent model was applied to calculate the air flow and heat transfer in the built-in PV-Trombe wall. The detailed equations for RNG k- ϵ turbulent model are described in Ref. [21, 22].

Discrete Ordinate (DO) radiation model was used to calculate the radiation heat transfer between the glass and the PV cells. A structured, mapped mesh with quadrilateral 2D elements was built in the code. The enhanced wall treatment was selected due to the large changes of temperature and pressure gradient near the wall region. In order to ensure the accuracy of the numerical results, a grid independence study was performed by changing the number of the nodes in the horizontal and vertical direction. The inlet and outlet were set as pressure inlet and pressure outlet respectively, a constant, uniform heat flux was imposed on both glass cover and PV cells in this simulation. The second-order upwind differencing scheme was adopted for the convective terms of the momentum and energy transport equations, and the SIMPLE method was used to solve the momentum and continuity equations. The simulations were conducted using the commercial CFD code, FLUENT version 6.3 [23].

2.3. Dimensionless numbers for heat transfer rate and air flow rate

Dimensionless numbers are introduced to derive general expressions for heat transfer and air flow in the Trombe wall channel, including Nusselt number for the heat transfer rate, Reynolds number for the air flowrate and Rayleigh number associated with the cavity size and boundary conditions.

The local and average Nusselt number are defined as [18]:

$$Nu_x = \frac{h_x b}{k} = \frac{q_w b}{(t_x - t_a)k} \quad (1)$$

$$Nu = \frac{h_c b}{k} = \frac{q_w b}{(t_w - t_a)k} \quad (2)$$

Where h_c and h_x are the average and local heat transfer coefficient respectively, b is the channel width, $q_w = (q_1 + q_2)/2$, k is the air thermal conductivity, $t_w = (t_1 + t_2)/2$, t_1 and t_2 are the temperatures of two heated wall surfaces, t_x is the local average temperature of the two heated wall surfaces, t_a is the temperature of ambient/inlet air flowing into the cavity. In the present calculation, t_a was 20 °C.

The air flow rate through a tall cavity is represented by the Reynolds number, Re , and for two-dimensional flow, it is defined the hydraulic diameter of the channel, which is twice of the channel width, b .

$$Re = \frac{2Ub}{\nu} = \frac{2Q}{\nu} \quad (3)$$

Where U is the average air velocity, Q is the flow rate for a unit length of two-dimensional cavity and ν is the kinematic viscosity of air.

A modified Rayleigh number is defined as the following, which takes into account the effect of the channel size and heat input into the channel,

$$Ra^* = \frac{g\beta q_w b^4}{\nu\alpha k H} \quad (4)$$

Where g is the gravitational acceleration, β and α are the thermal expansion coefficient and diffusion coefficient of air, respectively, H is the height of channel and b/H is the aspect ratio of channel.

3. Discussion of results

3.1. Validation of the numerical simulations

Gan [18] carried out CFD calculation on the ventilation and convective heat transfer in a traditional Trombe wall with the following parameters, $H=3\text{m}$, $b=0.1\text{m}-0.6\text{m}$ and the solar radiation, $S=100 \text{ W/m}^2$. We first conducted CFD calculation of the Trombe wall studied by Gan [18] and compared the present CFD results with the results by Gan [18] to validate the present modeling method. Figures 2 and 3 present the comparison. The present results agree well with the data by Gan [18] and the maximum error for the flow rate and average Nusselt number are only 6.9% and 10% respectively. The heat distribution ratio was defined as the ratio of the heat flux from the wall with the inlet (the right wall) to the total heat flux from both walls.

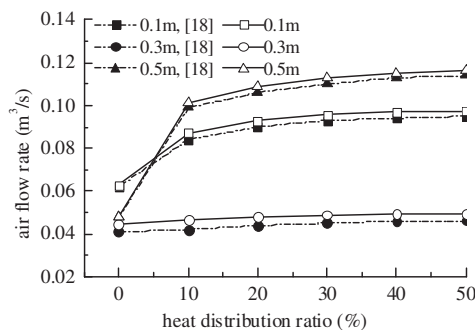


Figure 2 Air volume flow rate vs. heat distribution ratio

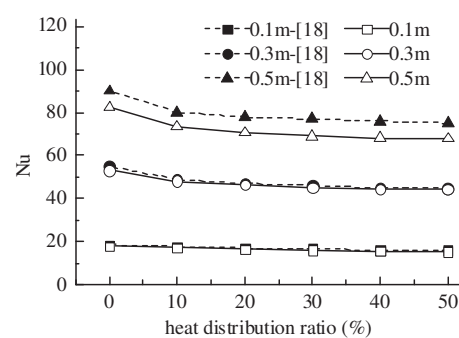


Figure 3 Average Nusselt number vs. heat distribution ratio

Moshfegh and Sandberg [24] experimentally investigated the air flow and heat transfer in a vertical channel made up of PV cells and insulated wall, which was actually used as a model of PV-Trombe wall, as showed in Figure 4. The sizes of the channel width, depth and height were 1.54m, 0.23m and 6.5m, respectively. The present CFD model was used to simulate the air flow in the vertical channel with the same sizes in the experiment conducted by Moshfegh and Sandberg [24]. The present CFD results of temperature difference of inlet and outlet air were compared with the experimental data by Moshfegh and Sandberg [24], as showed in Figure 4. Good agreement between the current results and reference data showed that the present model was reasonable for further calculation.

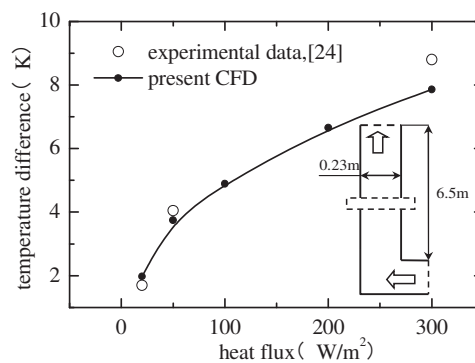


Figure 4 Comparison of experimental and numerical temperature difference of inlet and outlet air

3.2. Effect of channel width on air flow rate

Figure 5 presents the calculated air flow rate when the channel height is $H=2\text{m}$, 3m , 4m and the channel width increases from 0.1m to 0.9m . The air flow rate increased with the channel width to a maximum, then decreased as the channel width increased further. When the channel height increased, the channel width corresponding to the maximum flow rate increased. Therefore, there was an optimum aspect ratio for the Trombe wall design. In the present study, when $H=2\text{m}$, $(b/H)_{\text{opt}}=1/5$; $H=3\text{m}$, $(b/H)_{\text{opt}}=1/5$; $H=4\text{m}$, $(b/H)_{\text{opt}}=1/5$.

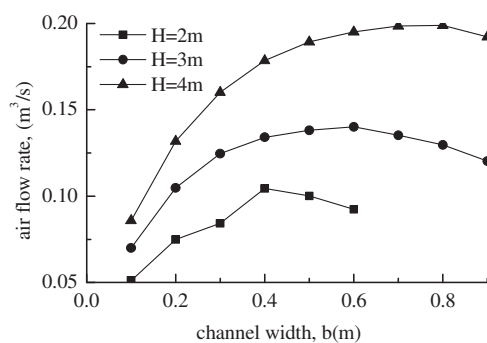


Figure 5 Air volume flow rate vs. channel width

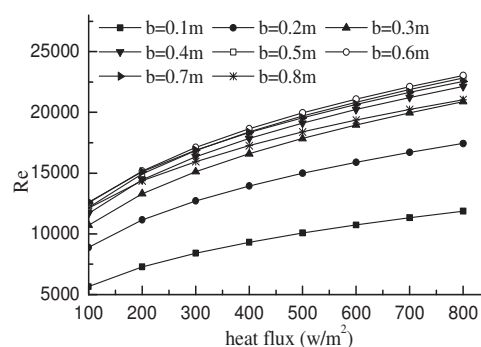


Figure 6 Re number vs. heat flux and channel width

Figure 6 presents the calculated Reynolds number when $H=3\text{m}$, $b=0.1\sim 0.8\text{m}$, $S=100\text{W/m}^2\sim 800\text{W/m}^2$. When the heat flux was given, Re increased first to a maximum then decreased as the channel width, b increased. When the channel width was given, Re increased with the heat flux, which explained that the ventilation was enhanced once more solar radiation was put into the Trombe wall channel.

3.3. Effect of channel width on heat transfer

Figure 7 presents the local Nusselt number along the channel height when $H=3\text{m}$, $S=400\text{W/m}^2$, $b=0.1\sim0.5\text{m}$. The local heat transfer was strong at the lower part in the channel and decreased to a constant along the height. This agreed with the development of the natural convection boundary layer over the wall surface along the height. The boundary layer was very thin at the lower part, so the local heat transfer was stronger. Figure 8 shows the average Nusselt number distribution when $H=3\text{m}$, $b=0.1\sim0.8\text{m}$, $S=100\text{W/m}^2\sim800\text{W/m}^2$. The average Nusselt number increased with both the heat flux and the channel width, as showed in Figure 8.

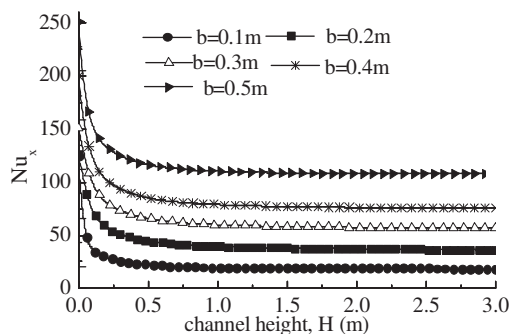


Figure7 Effect of channel width on local Nusselt number ($S=400\text{ W/m}^2$)

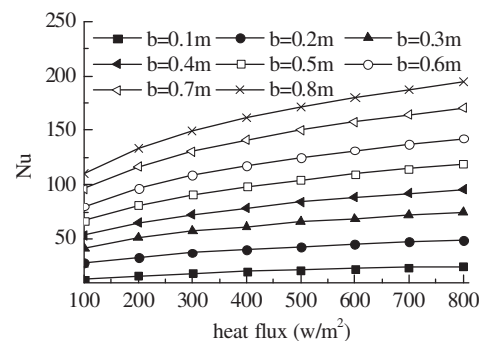


Figure8 Average Nusselt number vs. heat flux and channel width ($H=3\text{ m}$)

3.4. Effect of channel width on PV efficiency

The sunlight-electricity conversion efficiency of the PV cell depends on its surface temperature and could be calculated by the following equation [25]:

$$\eta_{cell} = \eta_0 [1 - 0.0045 \times (T_p - 298.15)] \quad (5)$$

Where η_0 is the efficiency at standard test condition, T_p is the average PV cell surface temperature.

When the channel width increased, the air flow behavior was influenced, which had an effect on the convection heat transfer over the PV cell surface, resulting to changed PV surface temperature. The multi-crystalline silicon cell was selected as the PV model and its physical properties were used for the calculation. When the channel height $H=3\text{ m}$, the solar radiation $S=400\text{ W/m}^2$, the calculated PV surface temperature and the efficiency were listed in Table 2.

Table 2 Average PV surface temperature and the PV efficiency

Channel width (m)	0.1	0.2	0.3	0.4	0.5	0.6	0.7
T_p (K)	348.9	351.9	346.5	346.8	346.9	345.6	345.1
Efficiency (%)	9.26	9.10	9.39	9.37	9.37	9.44	9.46

Compared to the efficiency at standard test condition for monocrystalline silicon cell, 12%, the PV cell efficiency in the PV-Trombe wall channel decreased by 20%-24%. As the channel width increased, the PV cell efficiency increased, because the air flow rate increased with the channel width, which improved the cooling of the PV surface.

3.5. Correlation for heat transfer and air flow rate

The average Nusselt number and the Reynolds number calculated when the channel height $H=3\text{m}$, the channel width $b=0.1\sim0.8\text{m}$, and the solar radiation $S=100\sim800\text{W/m}^2$, were plotted with the modified Rayleigh number, as showed in Figures 9 and 10. Log linear relations were found to exist between the

averaged Nu , Re and Ra^* value, as showed in Figures 9 and 10. A multivariable regression analysis was used to correlate the calculated results of the total 8×8 cases and the following dimensionless correlations were derived. These expressions will allow the calculation of the heat transfer rate/coefficient and air flow rate in a built-in PV-Trombe wall channel with vertical inlet for given channel size and solar radiation.

$$Nu = 1.3Ra^{*0.191} (R^2 = 0.922) \quad (6)$$

$$Re = 3164.6Ra^{*0.079} (R^2 = 0.922) \quad (7)$$

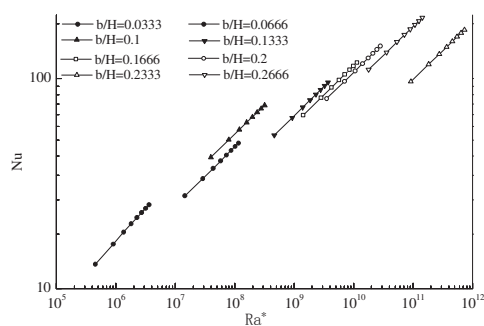


Figure 9 Nusselt number vs. Ra^*

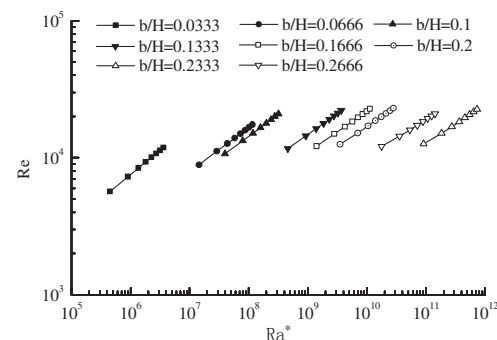


Figure 10 Reynolds number vs. Ra^*

4. Conclusion

The heat transfer and air flow in a built-in PV-Trombe wall channel were numerically simulated based on CFD and the effect of the channel width was discussed. Results showed that the air flow rate increased with the channel width to a maximum, then decreased as the channel width increased further. The optimum aspect ratio of the channel, $(b/H)_{opt}$ for the maximum flow rate was 1/5. The average Nusselt number increased with both the heat flux and the channel width. Dimensionless analysis showed that there was a log linear relation between the averaged Nu , Re and Ra^* value. Based on the calculated data from the total 8×8 cases, dimensionless correlations were derived for the calculation of the heat transfer and flow rate.

Acknowledgment

This work was supported by National Natural Science Foundation of China (No. 51278095 and No. 50806049), which are gratefully acknowledged.

References

- [1] Su Y and Liu Z 2011 *Sci. Rev. Tech.* **29**(27) 67-72
- [2] Saadatian O, Sopian K, Lim C H, Asim N, Sulaiman M Y 2012 *Renew. Sustain. Energy Rev.* **16** 6340- 51.
- [3] Bojic M, Johannes K, Kuznik F 2014 *Energy Build.* **70** 279-86
- [4] Abbassi F, Dimassi N, Dehmani L 2014 *Energy Build.* **80** 302-08
- [5] Briga-SáA, Martins A, Boaventura-Cunha J, Lanzinha J C, Paiva A 2014 *Energy Build.* **74** 111-19
- [6] Shen J, Lassue S, Zalewski L, Huang D 2007 *Energy Build.* **39** 962-74

- [7] Jaber S and Ajib S 2011 *Sol. Energy* **85** 1891–98
- [8] Ji J, Yi H, He W, Pei G, Lu J, Jiang B 2007 *Build. Environ.* **42** 1544-52
- [9] Ji J, Yi H, Pei G, Lu J 2007 *Appl. Therm. Eng.* **27** 1507-15
- [10] Ji J, Yi H, Pei G, Jiang B, He W *Build. Environ.* **42** 3529-39
- [11] Himanshu D 2009 *Sol. Energy* **83** 1933–42
- [12] Jiang B, Ji J, Yi H 2009 *Renew. Energy* **33** 2491-98
- [13] Sun W, Ji J, Luo C, He W 2011 *Appl. Energy* **88** 224-31
- [14] Koyunbaba B K, Yilmaz Z 2012 *Renew. Energy* **45** 111-18
- [15] Su Y, Zhao B, Xu X 2014 *Chem. Eng. Trans.* **39** 1489-94
- [16] Ong K S and Chow C C 2003 *Sol. Energy* **74** 1-17
- [17] Gan G 1998 *Energy Build.* **27** 37-43
- [18] Gan G 2011 *Build. Environ.* **46** 2069-80
- [19] Gan G 2006 *Energy Build.* **38** 410-20
- [20] Gan G 2010 *Build. Environ.* **45** 1173-83
- [21] Yakhot V, Orzsag S A 1986 *J. Sci. Comput.* **1** 1–51
- [22] Long T, Su Y, Xiang W, He C 2007 *Computational Fluid Dynamics* (Chongqing: Chongqing University Press)
- [23] FLUENT user's guide. 2006 (New Hampshire, USA: Fluent Inc)
- [24] Moshfeg B and Sandberg M 1998 *Renew. Sus. Energy Rev.* **2** 287-301
- [25] Zondag H A, De Vries D W, Van Helden WGJ 2002 *Sol. Energy* **72** 113-28